

# Galaxy-QSO correlation induced by weak gravitational lensing arising from large-scale structure

Antonio C. C. Guimarães<sup>1</sup>, Carsten van de Bruck<sup>2</sup>, and Robert H. Brandenberger<sup>1</sup>

<sup>1</sup>*Department of Physics, Brown University, Providence, RI 02912, USA; guimar@het.brown.edu*

<sup>2</sup>*DAMTP, Center for Mathematical Sciences, Wilberforce Road, CB3 0WA, Cambridge, U.K.*

4 October 2000

## ABSTRACT

Observational evidence shows that gravitational lensing induces an angular correlation between the distribution of galaxies and much more distant QSOs. We use weak gravitational lensing theory to calculate this angular correlation, updating previous calculations and presenting new results exploring the dependence of the correlation on the large-scale structure. We study the dependence of the predictions on a variety of cosmological models, such as cold dark matter models, mixed dark matter models, and models based on quintessence. We also study the dependence on the assumptions made about the nature of the primordial fluctuation spectrum: adiabatic, isocurvature and power spectra motivated by the cosmic string scenario are investigated. Special attention is paid to the issue of galaxy biasing, which is fully incorporated. We show that different mass power spectra imply distinct predictions for the angular correlation, and therefore the angular correlation provides an extra source of information about cosmological parameters and mechanisms of structure formation. We compare our results with observational data and discuss their potential uses. In particular, it is suggested that the observational determination of the galaxy-QSO correlation may be used to give an independent measurement of the mass power spectrum.

**Key words:** gravitational lensing — large-scale structure of universe

## 1 INTRODUCTION

According to general relativity, light from distant objects such as quasars is affected by the large-scale distribution of the intervening masses, and, consequently, these act as gravitational lenses. A gravitational lens enlarges the solid angle of the source and conserves its surface brightness. So at the same time it brings to view faint objects (magnification bias) and dilutes their population density. These two antagonistic effects can generate either correlation or anticorrelation between the angular distribution of background and foreground objects (see e.g. Schneider, Ehlers & Falco 1992).

Several studies have explored the correlation between QSO's and galaxies at various wavelengths. For example, Bartelmann & Schneider (1994) found a statistically significant correlation between 1Jy sources and IRAS galaxies for quasars at high redshifts. Also, Benítez & Martínez-González (1997) reported statistically significant correlations between COSMOS/UKST galaxies and PKS radio quasars, and Benítez, Sanz & Martínez-González (2001) found positive correlations using radio-loud quasars from the 1Jy and Half-Jansky samples. These results were obtained for small angles on the sky (of the order of 10 arcmin). Re-

cently, Williams & Irwin (1998) investigated the correlation between QSO's from the LBQS catalog and galaxies from the APM survey and detected a significant positive angular correlation, ranging from scales of 10 arcmin to over a degree. For a more extended review of observational data see Benítez et al. (2001), Bartelmann & Schneider (2001), and Norman & Willians (2000).

An analytical theory of the galaxy-QSO correlation due to weak gravitational lensing was introduced by Bartelmann (1995), Dolag & Bartelmann (1997), hereafter B95 and DB97, and Sanz, Martínez-González & Benítez (1997), having as base the work by Kaiser (1992). We will review the theory briefly in Section 2. The predicted correlations between galaxies and QSO's agree reasonably well with some observations for angles below 10 arcmin. However, Williams & Irwin (1998) claim that for larger angular scales theory and observations differ by one order of magnitude for standard cosmological models such as cold dark matter (*SCDM*) and cold dark matter with a cosmological constant ( *$\Lambda$ CDM*).

Although this conclusion has to be tested with future observations, it is of importance to investigate the predictions of the galaxy-QSO correlation for a large class of cosmologies. The effect of bias, matter content and current ex-

arXiv:astro-ph/0010104v3 25 Jul 2001

pansion rate has to be investigated in detail. This will be the aim of this paper, where we keep the assumption that the weak lensing approximation is valid. Effects of higher order terms are not investigated here. These contributions were estimated recently by Williams (2000), and were shown to increase the amplitude by less than 10 per cent for nearby large-scale coherent structures. Our investigations show that the observations of correlations between QSOs and galaxies on large angular scales can provide independent information relevant to structure formation understanding, and are somewhat sensitive to the values of a set of cosmological parameters.

The paper is organized as follows. In Section 2 we review the theoretical formalism used. In Section 3 we present the cosmological models we consider in our investigation and study their predictions. The models include mixed dark matter and quintessence models, as well as isocurvature and cosmic string based models of structure formation. We analyze in detail the effect of several cosmological parameters on the galaxy-QSO correlation in a flat universe with cosmological constant and initial adiabatic fluctuations. We discuss our findings and some observational data in Section 4.

## 2 THEORETICAL FRAMEWORK

In this section we review the theory of the correlation between galaxies and QSOs based on weak gravitational lensing. We follow closely Bartelmann (1995) and Dolag & Bartelmann (1997). However, we extend the theory by allowing for a scale- and time-dependent bias, and by using an improved mass power spectrum (e.g. by taking into account the baryon density and properly evolving non-linear density fields).

### 2.1 Angular correlation definition and calculation

We define the angular correlation function  $\xi_{GQ}(\phi)$  between galaxies and high-redshift QSO's as

$$\xi_{GQ}(\phi) \equiv \left\langle \left[ \frac{n_Q(\vec{\theta})}{\bar{n}_Q} - 1 \right] \left[ \frac{n_G(\vec{\theta} + \vec{\phi})}{\bar{n}_G} - 1 \right] \right\rangle, \quad (1)$$

where  $n_Q$  and  $n_G$  are the QSO and galaxy densities (a bar over a quantity indicates its mean value), and  $\langle \rangle$  represents the average over  $\vec{\theta}$  and the direction of  $\vec{\phi}$  (but not its modulus). Assuming weak gravitational lensing (i.e. that the magnification field contrast  $\delta\mu$  is small,  $|\delta\mu| \ll 1$ ), and a brightness distribution of the cumulative quasar number density as a function of flux  $S$  of the form  $n_Q(> S) \propto S^{-s}$ , one can show (B95) that

$$\xi_{GQ}(\phi) = (s-1) \langle \delta\mu(\vec{\theta}) \delta_{gal}(\vec{\theta} + \vec{\phi}) \rangle, \quad (2)$$

where  $\delta_{gal}$  is the galaxy density contrast.

The magnification fluctuations  $\delta\mu$  derive from the inhomogeneities in the mass distribution, since these create a gravitational potential topography which deflects light, and therefore generates a shear field. The calculation of this shear field (which assumes a statistically homogeneous and isotropic density field and a Newtonian weak field approximation for gravity), and the results involving the power spectra of projections of three-dimensional fields, obtained

by Kaiser (1992), allows one to derive the expression [equation (12) of DB97 generalized for a scale and time dependent bias factor  $b(k, w)$  (Benítez & Sanz 1999)]

$$\frac{\xi_{GQ}(\phi)}{s-1} = \frac{3\Omega_m}{2\pi(c/H_0)^2} \int_0^{w_\infty} dw \frac{W_G(w) G_Q(w)}{a(w)} \times \int_0^\infty dk k b(k, w) P_\delta(k, w) J_0[f_K(w)k\phi], \quad (3)$$

where  $w$  is the comoving distance which here parameterizes time ( $w_\infty$  represents a redshift  $z = \infty$ ), and  $k$  is the wavenumber of the density contrast in a plane wave expansion;  $\Omega_m$  is the matter density parameter;  $P_\delta(k, w)$  is the time evolved mass power spectrum;  $J_0$  is the zeroth-order Bessel function of first kind; and  $f_K(w)$  is the curvature-dependent radial distance ( $= w$  for a flat universe).

The scale factor,  $a = 1/(1+z)$ , is determined by solving the following integral equation for  $a$

$$w(a) = \int_a^1 \frac{da'}{a'^2 H(a')/H_0} \quad (4)$$

where  $H(a) = H_0 [\Omega_\Lambda(1-a^{-2}) + \Omega_m(a^{-3}-a^{-2}) + a^{-2}]^{1/2}$ . For an Einstein-de Sitter Universe ( $\Omega_m = 1$  and  $\Omega_\Lambda = 0$ ) the last equation can be easily solved, implying  $a(w) = (1-w/2)^2$ ,  $w$  being measured in units of  $c/H_0$ . For a general cosmology equation (4) has to be solved numerically.

The information about galaxy and QSO redshift distribution enters through the weight functions  $W_G(w)$  and  $G_Q(w)$ , respectively. We take  $W_G(w)$  from Kaiser (1992) with parameters  $\alpha = 1$ ,  $\beta = 4$  and a mean galaxy redshift  $z_G = 0.2$ , that is just a distribution sharply peaked at  $z_G$ , which mimics the APM survey redshift distribution well. For the QSO redshift distribution we adopt a simple linear ramp function which starts at a high value at a minimum redshift  $z_0 = 0.3$ , and falls to zero at  $z = 3.5$ . This also well mimics QSO surveys such as LBQS and PKS. From this distribution the QSO weight function  $G_Q(w)$  is calculated following DB97. Note however that the exact shape of these distributions is not crucial for our results, and its role is already discussed in B95.

### 2.2 Mass power spectrum

We define the linear mass power spectrum as usual

$$\Delta^2(k, w) \equiv \frac{k^3}{2\pi^2} P_\delta(k, w) = A \left( \frac{ck}{H_0} \right)^{3+n} T^2(k, w) D^2(w), \quad (5)$$

where  $A$  is the normalization factor<sup>\*</sup>;  $n$  is the initial power spectrum index (for a Harrison-Zel'dovich spectrum  $n = 1$ );  $T(k, w)$  is the transfer function; and  $D(w)$  is the growth function which we define as

$$D(w) = a \frac{g(a)}{g(1)}, \quad (6)$$

<sup>\*</sup>  $A = \delta_H$  if we normalize to COBE (Bunn & White 1997). Another possibility is to normalize to the cluster abundance (Viana & Liddle 1999), which would be in principle the most appropriate for our calculations, because it normalizes the power spectrum on scales that are relevant to weak lensing, while a normalization to the cosmic microwave background anisotropies does the normalization on much larger scales.

where  $a = a(w)$ , and  $g(a)$  is the linear growth suppression factor which is well approximated by (Carroll, Press & Turner 1992; Lahav et al. 1991)

$$g(a) = \frac{5}{2}\Omega_m(a) \left[ \Omega_m^{4/7}(a) - \Omega_\Lambda(a) \right] + \left( 1 + \frac{1}{2}\Omega_m(a) \right) \left( 1 + \frac{1}{70}\Omega_\Lambda(a) \right)^{-1}, \quad (7)$$

$$\Omega_m(a) = \frac{\Omega_m}{a^3} \left( \frac{H_0}{H} \right)^2, \quad (8)$$

$$\Omega_\Lambda(a) = \Omega_\Lambda \left( \frac{H_0}{H} \right)^2. \quad (9)$$

For an Einstein-de Sitter Universe  $g(a) = 1$  (no suppression of gravitational clustering), and the growth function reduces to the scale factor,  $D(w) = a(w)$ .

For CDM we use the transfer functions given by Bardeen et al. (1986), calculated with the shape parameter by Sugiyama (1995),  $\Gamma = \Omega_m h \exp[-\Omega_b(1 + \sqrt{2h/\Omega_m})]$ , where  $\Omega_b$  is the baryon energy density.

A realistic model for the mass power spectrum has to consider non-linear effects in the evolution of the density fields, important at small scales. One way to do this is by computer-intensive simulations, another is to use an approximate analytical form such as a scaling equation mapping the linear spectra to the non-linear one (Hamilton et al. 1991, Scranton & Dodelson 2000)

$$\Delta_{NL}^2(k_{NL}, w) = f_{NL}(\Delta_L^2(k_L, w)) \quad (10)$$

$$k_{NL} = k_L \left[ 1 + \Delta_{NL}^2(k_{NL}, w) \right]^{1/3}. \quad (11)$$

Expressions for the function  $f_{NL}(x)$  are given by Peacock & Dodds (1996) and Ma (1998), hereafter PD96 and Ma98. In the linear regime ( $x \ll 1$ )  $f_{NL}(x) \approx x$ , during the stable clustering regime ( $x \gg 1$ )  $f_{NL}(x) \propto x^{3/2}$ , and in the intermediate region ( $x \approx 1$ )  $f_{NL}(x)$  is extracted from N-body simulations.

## 2.3 Galaxy biasing

The simplest bias relation one can assume is linear and deterministic, so that one could define the bias as

$$b = \frac{(\sigma_8)_{gal}}{(\sigma_8)_{mass}}, \quad (12)$$

where

$$\sigma^2(R) = \int_0^\infty W^2(kR) \Delta^2(k) \frac{dk}{k}, \quad (13)$$

and  $W(x) = 3[\sin(x) - x \cos(x)]/x^3$ . Evaluated at  $R = 8h^{-1} Mpc$ , this gives  $\sigma_8$ . The subscripts ‘gal’ and ‘mass’ refer to the galaxy and mass power spectra.

However, the linear deterministic bias is a too simplistic model (Dekel & Lahav 1999). The most general biasing between galaxy and mass density contrasts that one can imagine is a non-linear stochastic bias which can be time- and scale-dependent:

$$\delta_{gal} = b(\delta)\delta + \epsilon, \quad (14)$$

where  $\epsilon$  is a random field.

From equation (2) we get that

$$\frac{\xi_{QG}(\phi)}{(s-1)} = \langle \delta\mu(\vec{\theta}) b[\delta(\vec{\theta} + \vec{\phi})] \delta(\vec{\theta} + \vec{\phi}) \rangle + \langle \delta\mu(\vec{\theta}) \epsilon(\vec{\theta} + \vec{\phi}) \rangle. \quad (15)$$

If we make the reasonable assumptions that  $\epsilon$  is independent of  $\delta\mu$  and has zero mean, then the last term on the right is clearly zero<sup>†</sup>, so a stochastic component of the biasing does not alter the expected value for the galaxy-QSO correlation.

To be most general, we further consider a scale- and time-dependent bias factor, which we assume can be written as  $b(k, w) = b_s(k)b_t(w)$ . The scale-dependent part of the bias is defined as

$$b_s(k) = \sqrt{\frac{P_{gal}(k)}{P_\delta(k)}}, \quad (16)$$

where  $P_{gal}(k)$  is an empirical galaxy power spectrum. We use (unless indicated) the spectrum obtained from the APM survey (Gaztañaga & Baugh 1998). The time-dependent part of the bias can be modeled as (Tegmark & Peebles 1998)

$$b_t(w) = \frac{\sqrt{(1-D)^2 - 2(1-D)r_0b_0 + b_0^2}}{b_0D}, \quad (17)$$

where  $b_0$  is the linear bias factor today (equation [12]),  $r_0$  is the dimensionless correlation coefficient between the distributions of mass and galaxies, and  $D = D(w)$  (equation [6]). However, we found that the time dependence is negligible (even considering a galaxy population at a higher redshift and a strong time dependence of the bias the effect is very small), so for simplicity one can neglect it.

## 3 RESULTS

In this section (except for Section 3.4) we explore the dependence of the galaxy-QSO angular correlation on several cosmological parameters, assuming structure formation from initial adiabatic fluctuations.

### 3.1 Three historical models

Fig. 1 shows our results for three cosmological models that were in fashion at some point in history, the ‘standard’ cold dark matter (*SCDM*:  $\Omega_m = 1$ ,  $h = 0.5$ ), a flat universe with a cosmological constant ( $\Lambda$ CDM:  $\Omega_m = 0.3$ ,  $\Omega_\Lambda = 0.7$ ,  $h = 0.7$ ), and an open universe (*OCDM*:  $\Omega_m = 0.3$ ,  $\Omega_\Lambda = 0$ ,  $h = 0.7$ ). It uses the COBE normalized mass power spectrum for these models, the necessary bias to match the APM galaxy power spectrum (equation [16]), and the calculated galaxy-QSO angular correlation (equation [3]). The three cosmological models are clearly differentiated by the predicted  $\xi_{GQ}(\phi)$ .

A normalization of the power spectrum to the cluster abundance simply rescales our results for  $\xi_{GQ}(\phi)$  by  $(\sigma_8)_{cluster}/(\sigma_8)_{COBE}$ . The resulting correlations decrease for *SCDM*, increase for *OCDM*, and remain the same for  $\Lambda$ CDM, making the differentiation among the models less evident.

The latest CMB observation (Bernardis et al. 2000, and

<sup>†</sup> While this is certainly true for averages over large angular regions, for patches smaller than the typical scales of variation of the fields involved this term could contribute because of statistical variance.

Hanany et al. 2000) point to a flat universe, as favored by most inflationary models. The result of these observations, and the suggestion of the existence of a dark energy component by supernova observations, strongly induce one to take  $\Omega \equiv \Omega_m + \Omega_\Lambda = 1$ . This flat universe with low matter density (most of it coming from some sort of cold dark matter), dark energy (cosmological constant or quintessence), and adiabatic fluctuations with an initial spectrum nearly scale-free, constitutes the most popular cosmological model today. We will concentrate on this model, searching for the effects of variations of the cosmological parameters around the most likely values.

### 3.2 Adiabatic flat universe with $\Lambda$

The matter density parameter  $\Omega_m$  enters the calculation of  $\xi_{GQ}(\phi)$  at several levels. It is a multiplicative factor of the whole expression in equation (3), it determines the general geometric scaling of the problem through the scale factor, and it also enters in the mass power spectrum (and consequently in the bias, too) through the shape parameter, the growth function, and normalization.

We investigate the dependence of the galaxy-QSO correlation on the matter content of a flat universe in Fig. 2. As would be expected, a higher matter content generates more power of the mass spectrum on small scales, which results in a higher correlation between galaxies and QSO's (mainly at small angles).

Recent experiments give extra support to the possibility that neutrinos are massive. This necessarily implies a hot dark matter (HDM) component to the matter content of the universe, because theory predicts a cosmic neutrino background of temperature 1.95 K. A pure HDM universe is ruled out, because it would not have the observed amount of structure on small scales, as they are suppressed by free streaming. However, a mixed dark matter scenario (MDM) with a small fraction of HDM is possible.

We calculate  $\xi_{GQ}(\phi)$  in a MDM universe using the linear mass power spectrum derived by Ma (1996) and obtain the full non-linear time evolved spectrum using the prescription by Ma (1998), which properly takes into account the time evolution of the hot and cold dark matter components (the PD96 prescription does not give the correct result in this case). Fig. 3 shows our results. The larger the fraction of HDM over CDM, the larger the suppression of structures on small scales. A large neutrino energy density  $\Omega_\nu$  results in less power at large  $k$ . The consequence on  $\xi_{GQ}(\phi)$  is a lower correlation at small angles (and a flatter general slope).

The baryon density of the universe is fairly well determined (Burles et al. 1999) and represents a small fraction of the total matter. In our calculations  $\Omega_b$  enters through the shape parameter  $\Gamma$  of the transfer function. This is just an approximation, because it does not account for baryonic oscillations (Eisenstein & Hu 1998), but it is good enough for low values of  $\Omega_b$ . We studied the influence of a baryonic content varying from 0 to 8 per cent of the critical density on the galaxy-QSO correlation (see Fig. 4). A higher baryon density implies less power on small scales for the mass spectrum and a lower value of  $\xi_{GQ}(\phi)$  on small angles.

Inflation favors an initial power index  $n \approx 1$  for the spectrum of density fluctuations, but some degree of 'tilting' is possible depending of the inflationary theory. We look at

the effect of modifying the initial power spectrum index by simple tilting at Fig. 5. A higher  $n$  implies a steeper  $\xi_{GQ}(\phi)$ , since it induces more power on small scales.

The effect of a Hubble parameter in the range  $0.5 < h < 0.8$  on the predicted  $\xi_{GQ}(\phi)$  was also considered. A higher value for  $h$  implies a higher correlation, as also previously shown in DB97.

### 3.3 Quintessence

One alternative for the cosmological constant as dark energy is a dynamical and spatially homogeneous (on cluster scales) field, or, as it has been called, quintessence (see e.g. Wetterich 1988, Ratra and Peebles 1988). Such a field has negative pressure and an equation of state  $p = \omega_Q \rho$  with coefficient in the range  $-1 \leq \omega_Q < 0$ . We implement a quintessence model (*QCDM*) with constant  $\omega_Q$  by generalizing the time dependent Hubble expansion rate to

$$H(a) = H_0 [\Omega_Q (a^{-3(\omega_Q+1)} - a^{-2}) + \Omega_m (a^{-3} - a^{-2}) + a^{-2}]^{1/2}, \quad (18)$$

and by using the results of Ma et al. (1999) for the construction of the fully evolved non-linear mass power spectrum. Note that  $\omega_Q = -1$  reduces everything to the case of a cosmological constant.

Our results are shown in Fig. 6. A greater  $\omega_Q$  (closer to 0) implies a lower amount of large-scale structures over small ones in the relevant range (at much larger scales the clustering of the quintessence field becomes important), which results in a steeper slope for  $\xi_{GQ}(\phi)$ . The same conclusion is valid if we normalize the *QCDM* spectra to the cluster abundance, which also depends on  $\omega_Q$  according to Wang & Steinhardt (1998). Note that, because the larger scale structures are the most affected by the coefficient of the quintessence equation of state, the effect on the correlation is more dramatic at large angles.

### 3.4 Alternatives for structure formation

We also investigated alternatives to adiabatic fluctuations as mechanism for structure formation: isocurvature fluctuations and the cosmic strings scenario.

A general treatment of initial perturbations allows the existence of isocurvature modes (Bucher, Moodley, & Turok 2000). We consider an isocurvature CDM model for the mass power spectrum using the transfer function by Bardeen et al. (1986) and the spectral index obtained by Peebles (1999). In this case we use PD96 to obtain the non-linear spectrum and normalize it to the cluster abundance.

Except for inflationary models, topological defect models are the only known way of seeding structure formation (see e.g. Vilenkin and Shellard 1994, Hindmarsh and Kibble 1995, and Brandenberger 1994 for recent reviews). We explore this scenario for structure formation through the mass power spectrum generated by a network of cosmic strings (Avelino, Caldwell & Martins 1997). Note that the formalism used is insensitive to deviations from Gaussianity. Such deviations are a common feature of cosmic strings scenarios. Again, the non-linear spectrum is obtained by PD96 prescription and is CMB-normalized, which implies  $\sigma_8 = 0.46$ . A normalization to the cluster abundance requires  $\sigma_8 = 0.81$  [see Avelino, Wu & Shellard (2000); a somewhat smaller normalization was obtained by van de Bruck (1999)].

Both scenarios are in serious trouble if considered as the only mechanism responsible for structure formation. However, hybrid models are still allowed and maybe even favored by the first results from the Boomerang data (Bernardis et al. 2000) which yields an indication of a low amplitude for the secondary acoustic peak. See Bouchet et al. (2000), Battye & Weller (2000), and Avelino, Caldwell & Martins (1999) for considerations on hybrid models with topological defects, and Enqvist, Kurki-Suonio & Valiviita (2000) for limits on isocurvature fluctuations from CMB anisotropies. Our results for these two alternative models for structure formation are compared with the adiabatic case in Fig. 7. Both predict a steeper slope for  $\xi_{GQ}(\phi)$  than adiabatic fluctuations. This is because their power spectra have more power on smaller scales relative to large ones than the adiabatic spectrum.

#### 4 DISCUSSION

We studied in detail the role of several cosmological parameters and models of structure formation on the prediction of the angular correlation between galaxies and QSOs induced by weak gravitational lensing.

In a log-log plot  $\xi_{GQ}(\phi)$  can be roughly characterized by an amplitude and a slope. The amplitude is closely related to the normalization of the mass power spectrum, and the slope to its shape. More power on small scales (large  $k$ ) implies a steeper slope. This is a reflection of the fact that the amount of small scale structure is responsible for the galaxy-QSO correlation on small angles and larger structures are responsible for the correlation on larger angles. This simplicity of behavior results in a relatively large degeneracy of  $\xi_{GQ}(\phi)$  as a function of the cosmological parameters and models analyzed. In brief, a higher value of  $\Omega_m$ ,  $n$ , or  $h$  has nearly the same effect on  $\xi_{GQ}(\phi)$  as a lower value of  $\Omega_\nu$ , or  $\Omega_b$ . This effect is a higher correlation on small angles. Roughly, this represents a steeper slope for  $\xi_{GQ}(\phi)$ , which can be also achieved by shifting  $\omega_Q$  closer to zero, or by introducing an isocurvature or cosmic string component.

The main lesson given by the use of different theoretical mass power spectra is that the galaxy-QSO correlation at different angles contains information about the amount of structure at different scales.

Our calculations fully incorporate galaxy biasing. This requires the use of an empirical galaxy power spectrum. We choose to use the spectrum obtained from the APM survey, but this choice is not unique. Spectra from other surveys are available and could be used as well. These spectra do not all agree (see Einasto et al. 1999), allowing some freedom for the galaxy-QSO correlation prediction, because our  $\xi_{GQ}(\phi)$  calculation can be seen as an integral over an effective mean spectrum  $\sqrt{P_{gal}(k)P_s(k)}$ . In a similar way, the use of a power spectrum of cluster of galaxies allows for a prediction of the correlation between galaxy clusters and QSOs. To illustrate this point we use the spectrum obtained from the Abell-ACO clusters of galaxies (Miller & Batuski 2001) as  $P_{gal}(k)$ . We show the effect of this alternative choice at Fig. 8, which gives a higher amplitude for  $\xi_{GQ}(\phi)$ , roughly given by a factor  $(\sigma_8)_{Abell-ACO}/(\sigma_8)_{APM} \approx 4$ , where  $(\sigma_8)_{Abell-ACO} = 3.2$  is the rms fluctuation for the Abell-ACO spectrum, and  $(\sigma_8)_{APM} = 0.82$ . The correlation

curve found using the Abell-ACO spectrum is also slightly steeper than that using APM, because the first spectrum is flatter than the second at large  $k$  [ $P_{Abell-ACO}(k) \propto k^{-1.2}$  and  $P_{APM}(k) \propto k^{-1.4}$ ].

We also plot in Fig. 8 some points obtained from observations. A direct comparison among the different data sets is not possible, because they were obtained from different QSO and galaxy populations. For the same reason a strict comparison between these observational points and the theoretical predictions shown is not possible. That would require an individual calculation for each of the data sets, which would take in account the different redshift distributions for QSOs and galaxies, and also the particular power spectrum of the foreground population (galaxies or galaxy groups). This would be necessary because when selection criteria are applied to a foreground object catalog the effective power spectrum of the resulting subset is possibly different from the spectrum of the whole population. A rigorous analysis of the data would also require considerations about observational particularities such as the possible effects of dust and systematics. That is not our aim here. Nevertheless, a qualitative agreement in behavior between data and predictions can be glimpsed.

Another way to analyze the results from the several groups (avoiding the messiness of noise data) is to capture the essence of each data set by adjusting a power law to each one. We find the best fit of  $\xi_{GQ}(\phi)/(s-1) = A(\phi/1')^B$  to the data by the least squares method (see Table 1). To compare with the predictions shown in Fig. 8 we can take the amplitude  $A$  as being the value of  $\xi_{GQ}(\phi)/(s-1)$  at  $\phi = 1'$  (for the Abell-ACO result  $A \approx 0.04$  and for APM  $A \approx 0.008$ ), and power index  $B$  as the average bi-log slope of  $\xi_{GQ}(\phi)/(s-1)$ , which gives  $B \approx -0.8$ . Note however that for  $\phi \lesssim 1'$  the weak lensing assumption is not satisfied (strong lensing becomes important), so that the predictions for  $\xi_{GQ}(\phi)$  are underestimated in this range.

Benítez & Martínez-González (1997) (BMG97) found the galaxy-QSO correlation for angles up to 15 arcmin using radio loud QSOs from the PKS catalog and also using optically selected QSOs from the LBQS catalog. For this last group there is a large dispersion of data and points with negative correlation on small angles were found; the overall result is a null correlation (dust and selection bias were mentioned as possible explanations). The large error bars obtained for the two quasar samples make these observations compatible with predictions. Benítez et al. (2001) (BSMG00) obtained a somewhat higher correlation on the same angular scales using quasars from the Half-Jansk and 1Jy samples.

Williams & Irwin (1998) (WI98) also used a subsample of the LBQS catalog to determine the galaxy-QSO correlation, but for larger angles (7 to 300 arcmin). For angles up to nearly 100 arcmin they find a much higher correlation than the predicted one, and for angles larger than that the correlation is dispersed around zero, being compatible with predictions. Croom & Shanks (1999) (CS99) reinterpreted the anti-correlation between faint QSOs and galaxy groups found by Boyle, Fong & Shanks (1988) as being due to gravitational lensing. A flat QSO number count ( $s = 0.78$ ) was used to explain the negative correlation, but a surprisingly high amplitude is obtained when  $\xi_{GQ}(\phi)/(s-1)$  is calculated. This high amplitude would be in concordance with a

higher normalization of the power spectrum of the galaxy groups. Other works also seek to find the observed galaxy-QSO correlation, but the general conclusion that one can reach is that up to now  $\xi_{GQ}(\phi)$  is an observationally not very well determined quantity.

The use of much larger catalogs (e.g. the Sloan Digital Sky Survey with  $\approx 10^5$  QSOs, and the 2dF survey) may allow a more precise and accurate measurement of  $\xi_{GQ}(\phi)$  which in turn may constitute an independent way for the determination of the mass power spectrum, and a valuable tool for investigating structure formation and large-scale structure.

## ACKNOWLEDGEMENTS

ACCG thanks Ian dell'Antonio for his valuable comments, and also the Rutgers University Physics Department for the occasional use of its facilities. C.vdB was supported by the Deutsche Forschungsgemeinschaft DFG (at Cambridge) and by NATO/DAAD (at Brown). The research at Brown was supported in part by the US Department of Energy under Contract DE-FG0291ER40688, Task A.

## REFERENCES

- Avelino P.P., Caldwell R.R., Martins C.J.A.P., 1997, Phys. Rev. D, 56, 4568  
 Avelino P.P., Caldwell R.R., Martins C.J.A.P., 1999, Phys. Rev. D, 59, 123509  
 Avelino P.P., Wu J.H.P., Shellard E.P.S., 2000, MNRAS, 318, 329 (astro-ph/9906313)  
 Bardeen J.M., Bond J.R., Kaiser N., Szalay A.S., 1986, ApJ, 304, 15  
 Bartelmann M., 1995, A&A, 298, 661 (B95)  
 Bartelmann M., Schneider P., 1994, A&A, 284, 1  
 Bartelmann M., Schneider P., 2001, Phys.Rep., 340, 291 (astro-ph/9912508)  
 Battye R.A., Weller J., 2000, Phys. Rev. D, 61, 043501  
 Benítez N., Martínez-González E., 1997, ApJ, 477, 27 (BMG97)  
 Benítez N., Sanz J.L., 1999, ApJ, 525, L1  
 Benítez N., Sanz J.L., Martínez-González E., 2001, MNRAS, 320, 241 (astro-ph/0008394) (BSMG00)  
 Bernardis P. et al., 2000, Nature, 404, 955  
 Bouchet F.R., Peter P., Riazuelo A., Sakellariadou M., 2000, preprint (astro-ph/0005022)  
 Boyle B.J., Fong R., Shanks T., 1988, MNRAS, 231, 897  
 Brandenberger R.H., 1994, Int. J. Mod. Phys. A, 2117  
 Bucher M., Moodley K., Turok N., 2000, Phys. Rev. D, 62, 83508 (astro-ph/9904231)  
 Bunn E.F., White M., 1997, ApJ, 480, 6  
 Burles S., Nollett K.M., Truran J.N., Turner M.S., 1999, Phys. Rev. Lett., 82, 4176  
 Carroll S.M., Press W.H., Turner E.L., 1992, ARA&A, 30, 499  
 Croom S.M., Shanks T., 1999, MNRAS, 307, L17 (astro-ph/9905249) (CS99)  
 Dekel, A., Lahav, O., 1999, ApJ, 520, 24  
 Dolag K., Bartelmann M., 1997, MNRAS, 291, 446 (DB97)  
 Einasto J. et al., 1999, ApJ, 519, 441  
 Eisenstein D.J., Hu W., 1998, ApJ, 496, 605  
 Enqvist K., Kurki-Suonio H., Valiviita J., 2000, Phys. Rev. D, 62, 103003 (astro-ph/0006429)  
 Gaztañaga E., Baugh C.M., 1998, MNRAS, 294, 229  
 Hamilton A.J.S., Kumar P., Lu E., Matthews A., 1991, ApJ, 374, L1

- Hanany S. et al., 2000, ApJ, 545, L5 (astro-ph/0005123)  
 Hindmarsh M., Kibble T.W.B., 1995, Rep. Prog. Phys. 58, 477  
 Kaiser N., 1992, ApJ, 388, 272  
 Lahav O., Lilje P.B., Primack J.R., Rees M.J., 1991, MNRAS, 251, 128  
 Ma C.-P., 1996, ApJ, 471, 13  
 Ma C.-P., 1998, ApJ, 508, L5 (Ma98)  
 Ma C.-P., Caldwell R.R., Bode P., Wang L., 1999, ApJ, 521, L1  
 Miller C.J., Batuski D.J., 2001, ApJ, 551, 635 (astro-ph/0002295)  
 Norman D.J., Willians L.L.R., 2000, ApJ, 119, 2060  
 Peacock J.A., Dodds S.J., 1996, MNRAS, 280, L19 (PD96)  
 Peebles P.J.E., 1999, ApJ, 510, 531  
 Ratra B., Peebles P.J.E., 1988, ApJ, 325, L17  
 Sanz J.L., Martínez-González E., Benítez N., 1997, MNRAS, 291, 418  
 Schneider P., Ehlers J., Falco E., 1992, Gravitational Lenses, Springer Verlag, Heidelberg  
 Scranton R., Dodelson S., 2000, preprint (astro-ph/0003034)  
 Sugiyama N., 1995, ApJS, 100, 281  
 Tegmark M., Peebles P.J.E., 1998, ApJ, 500, L79  
 van de Bruck C., 1999, in Klapdor-Kleingrothaus H.V., Baudis L., eds, Dark matter in astrophysics and particle physics, 1998, Proc. Second International Conf. Dark Matter in Astrophysics and Particle Physics. IOP Pub., Philadelphia, p. 17 (astro-ph/9810409)  
 Viana T.P., Liddle A.R., 1999, MNRAS, 303, 535  
 Vilenkin A., Shellard E.P.S., 1994, Strings and Other Topological Defects, Cambridge Univ. Press, Cambridge  
 Wang L., Steinhardt P.J., 1998, ApJ, 508, 483  
 Wetterich C., 1988, Nucl. Phys. B302, 688  
 Williams L.L.R., 2000, ApJ, 535, 37  
 Williams L.L.R., Irwin M., 1998, MNRAS, 298, 378 (WI98)

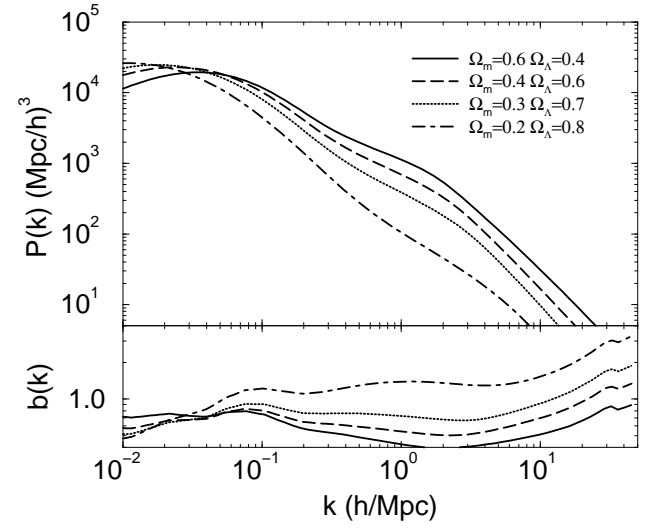
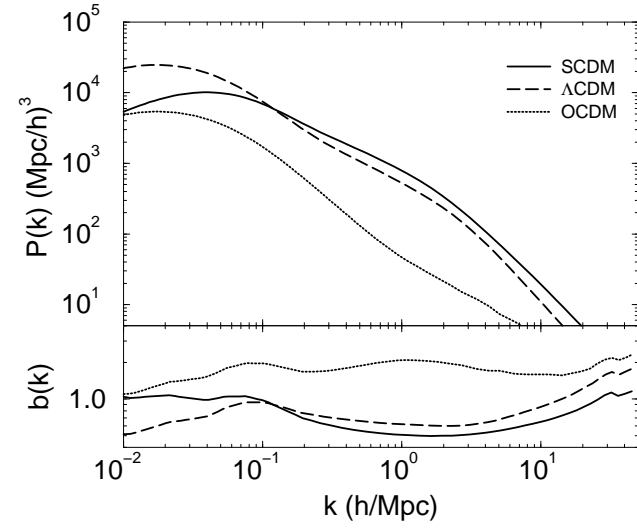


**Figure 1.** Three cosmological models. Non-Linear mass power spectrum (top graph), bias (central graph), and angular correlation  $\xi_{GQ}(\phi)/(s-1)$  (bottom graph). The internal plot is the result for the mass power spectrum normalized to the cluster abundance. Solid lines are for *SCDM*,  $\Omega_m = 1$ ,  $h = 0.5$  ( $\sigma_8 = 1.1$ ); dashed ones for  $\Lambda$ *CDM*,  $\Omega_m = 0.3$ ,  $\Omega_\Lambda = 0.7$ ,  $h = 0.7$  ( $\sigma_8 = 1.0$ ); and dotted ones for *OCDM*,  $\Omega_m = 0.3$ ,  $\Omega_\Lambda = 0$ ,  $h = 0.7$  ( $\sigma_8 = 0.46$ ). Other parameters are  $\Omega_b = 0.019/h^2$ ,  $n = 1$ , non-linear approximation by PD96.

**Figure 2.** Dependence on matter density in a flat universe with cosmological constant ( $\Omega_m + \Omega_\Lambda = 1$ ). Solid lines are for  $\Omega_m = 0.6$  ( $\sigma_8 = 1.4$ ); dashed ones for  $\Omega_m = 0.4$  ( $\sigma_8 = 1.2$ ); dotted ones for  $\Omega_m = 0.3$  ( $\sigma_8 = 1.0$ ); and dot-dashed ones for  $\Omega_m = 0.2$  ( $\sigma_8 = 0.72$ ). Other parameters are  $\Omega_b = 0.019/h^2$ ,  $h = 0.7$ ,  $n = 1$ , non-linear approximation by Ma98.

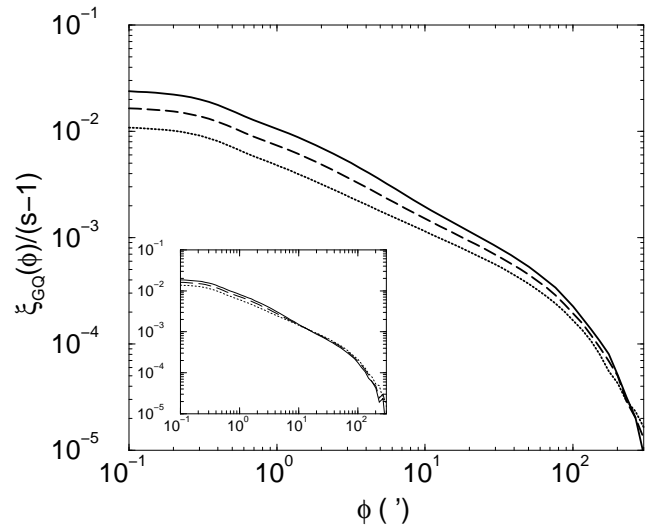
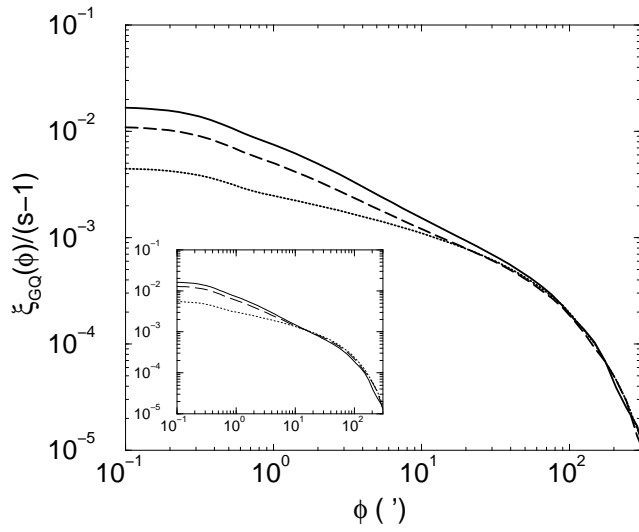
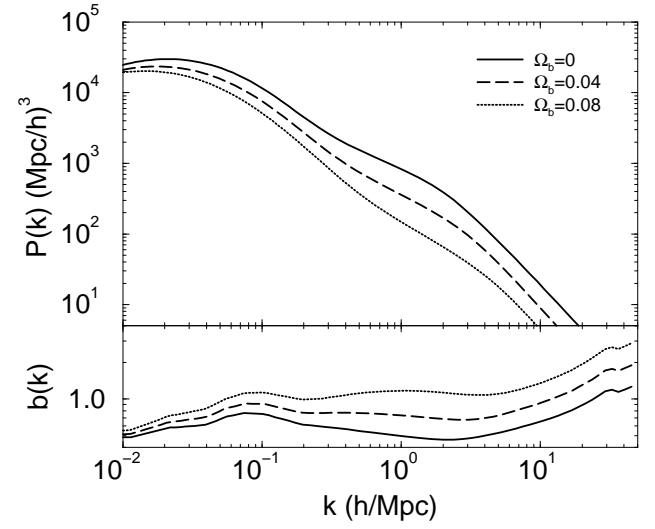
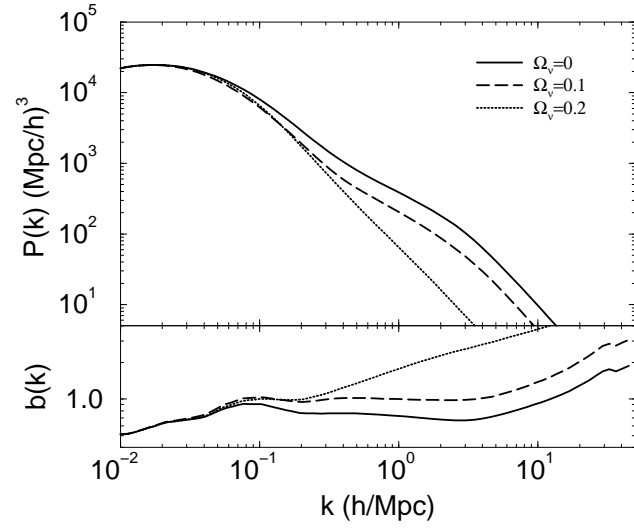


**Figure 3.** Dependence on hot dark matter density. Solid lines are for  $\Omega_\nu = 0$  ( $\sigma_8 = 1.0$ ); dashed ones for  $\Omega_\nu = 0.1$  ( $\sigma_8 = 0.84$ ); and dotted ones for  $\Omega_\nu = 0.2$  ( $\sigma_8 = 0.81$ ). Other parameters are  $(\Omega_m, \Omega_\Lambda, \Omega_b) = (0.3, 0.7, 0.019/h^2)$ ,  $h = 0.7$ ,  $n = 1$ , non-linear approximation by Ma98.

**Figure 4.** Dependence on baryon density. Solid lines are for  $\Omega_b = 0$  ( $\sigma_8 = 1.3$ ); dashed ones for  $\Omega_b = 0.04$  ( $\sigma_8 = 1.0$ ); and dotted ones for  $\Omega_b = 0.08$  ( $\sigma_8 = 0.79$ ). Other parameters are  $\Omega_m = 0.3$ ,  $\Omega_\Lambda = 0.7$ ,  $h = 0.7$ ,  $n = 1$ , non-linear approximation by Ma98.



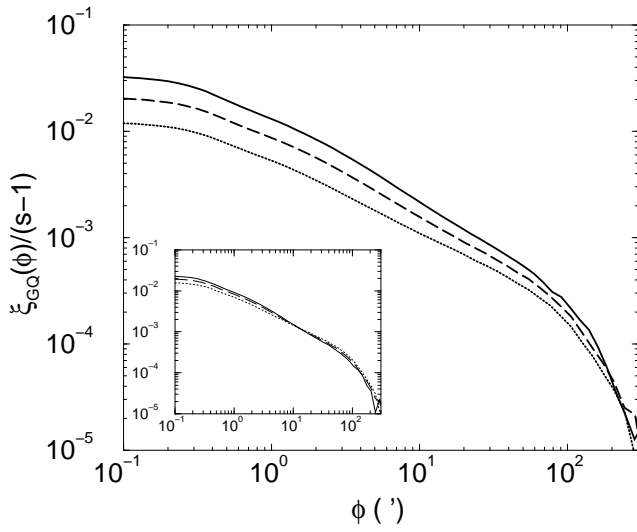
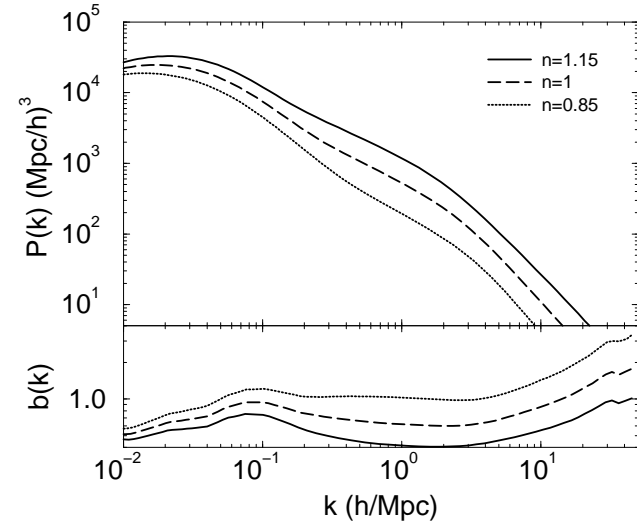


**Figure 5.** Dependence on the primordial spectral index. Solid lines are for  $n = 1.15$  ( $\sigma_8 = 1.4$ ); dashed ones for  $n = 1$  ( $\sigma_8 = 1.0$ ); and dotted ones for  $n = 0.85$  ( $\sigma_8 = 0.75$ ). Other parameters are  $(\Omega_m, \Omega_\Lambda, \Omega_b) = (0.3, 0.7, 0.019/h^2)$ ,  $h = 0.7$ , non-linear approximation by PD96.

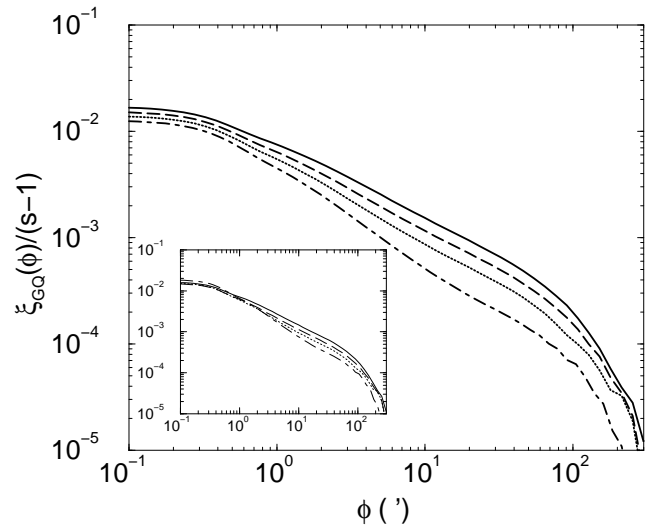
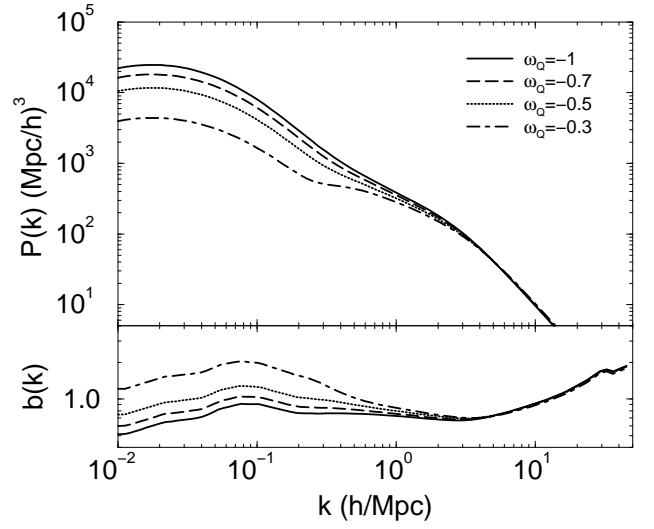


**Figure 6.** Quintessence. Solid lines are for  $\omega_Q = -1$  ( $\sigma_8 = 1.0$ ); dashed ones for  $\omega_Q = -0.7$  ( $\sigma_8 = 0.9$ ); dotted ones for  $\omega_Q = -0.5$  ( $\sigma_8 = 0.76$ ); and dot-dashed ones for  $\omega_Q = -0.3$  ( $\sigma_8 = 0.54$ ). Other parameters are  $(\Omega_m, \Omega_Q, \Omega_b) = (0.3, 0.7, 0.019/h^2)$ ,  $h = 0.7$ ,  $n = 1$ , non-linear approximation by Ma et al. (1999).

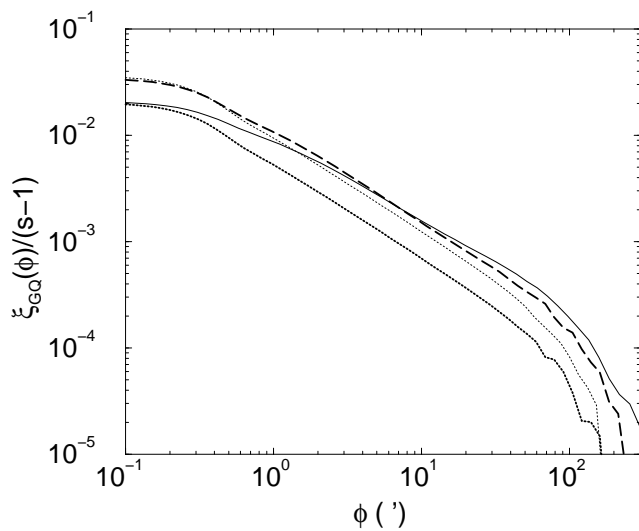
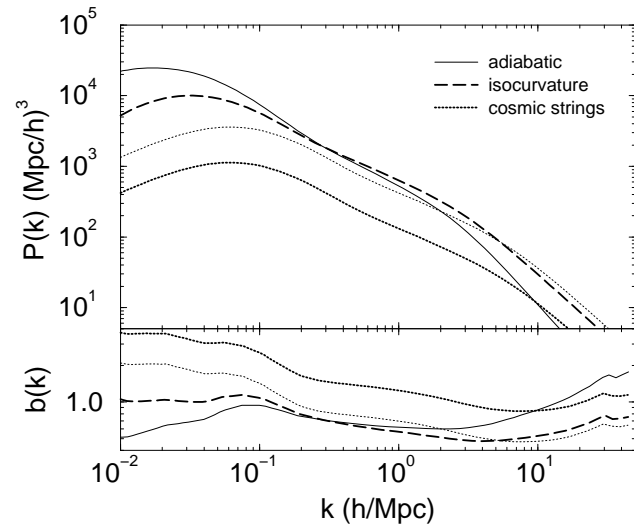


**Figure 7.** Alternative models for structure formation. Solid lines are for adiabatic fluctuations ( $n = 1$ ,  $\sigma_8 = 1.0$ ); dashed ones for isocurvature fluctuations ( $n = -1.8$ ,  $\sigma_8 = 0.99$ ); and dotted ones for cosmic strings ( $\sigma_8 = 0.46$ ). The thin dotted line corresponds to the normalization of the cosmic strings spectrum to the cluster abundance ( $\sigma_8 = 0.81$ ). Other parameters are  $\Omega_m = 0.3$ ,  $\Omega_\Lambda = 0.7$ ,  $\Omega_b = 0.019/h^2$  (cosmic strings results do not incorporate baryons),  $h = 0.7$ , non-linear approximation by PD96.

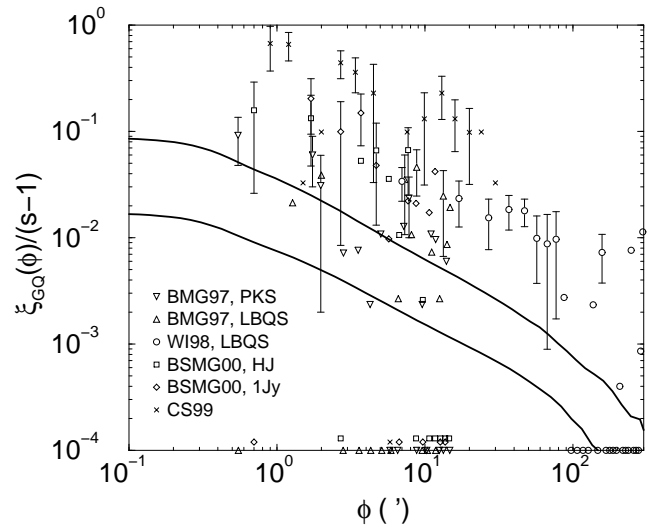


**Figure 8.** Predictions and some observational points. Solid lines are the theoretical predictions for a flat universe with cosmological constant and adiabatic fluctuations ( $\Omega_m = 0.3$ ,  $\Omega_\Lambda = 0.7$ ,  $\Omega_b = 0.019/h^2$ ,  $n = 1$ ,  $h = 0.7$ ,  $\sigma_8 = 1.0$ ). The upper curve uses the power spectrum from Abell-ACO (galaxy clusters), and the lower curve the APM survey (galaxies). Observational points are also plotted as an illustration. Some error bars would explode in the lower part if plotted, so we do not show them. The points close to the lower axis represent values of  $\xi_{GQ}(\phi)/(s-1)$  equal or less than zero. Note the caveats listed in the main text concerning the comparison among different data sets and theoretical predictions.

**Table 1.** Best fit to  $\xi_{GQ}(\phi)/(s-1) = A(\phi/1')^B$ , with  $B \leq 0$ .  $\phi$  is the angular range covered in arcmin, and  $N$  is the number of points. The uncertainties are given by the projection of the  $1\sigma$  confidence level contour, and (...) represents a large value outside the investigated parameter space. Values for  $s$  were taken from the respective papers.

data set	$s$	$\phi$ (')	N	$\chi^2$	$A$	$B$
BMG97, PKS	3.5	0.5–15	20	17.0	$0.05^{+0.03}_{-0.03}$	$-1.3^{+0.5}_{-(...)}$
BMG97, LBQS	2.5	0.5–15	20	19.0	$0.00^{+0.03}_{-0.07}$	$0.^{+0}_{-(...)}$
WI98, LBQS	2.75	7–300	30	40.1	$0.3^{+0.3}_{-0.2}$	$-1.0^{+0.2}_{-0.3}$
WI98, LBQS	2.75	7–100	10	3.83	$0.11^{+0.14}_{-0.07}$	$-0.6^{+0.3}_{-0.3}$
BSMG00, HJ	1.42	0.7–15	15	11.1	$0.1^{+0.1}_{-0.1}$	$-1.4^{+0.9}_{-(...)}$
BSMG00, 1Jy	1.93	0.7–15	15	13.7	$0.1^{+0.1}_{-0.1}$	$-1.^{+1}_{-(...)}$
CS99	0.78	0.9–30	15	14.5	$0.5^{+0.2}_{-0.2}$	$-0.6^{+0.2}_{-0.3}$